Climate Dynamics (2020) 54:4059–4074
https://doi.org/10.1007/s00382-020-05214-5

Planetary waves in the mesosphere lower thermosphere during stratospheric sudden warming: observations using a network of meteor radars from high to equatorial latitudes

N. Koushik[1] · K. Kishore Kumar[1] · Geetha Ramkumar[1] · K. V. Subrahmanyam[1] · G. Kishore Kumar[2] · W. K. Hocking[3] · Maosheng He[4] · Ralph Latteck[4]

Received: 11 July 2019 / Accepted: 13 March 2020 / Published online: 19 March 2020

Abstract
In the present communication, characteristics of mean winds and planetary waves in the mesosphere lower thermosphere (MLT) region during sudden stratospheric warming (SSW) events using observations from four meteor wind radars located at high, middle, low and equatorial latitudes are discussed. The response of the respective MLT regions to three SSW events that occurred during 2008–09, 2009–10 and 2011–12 winters are investigated. SSW signatures in the MLT zonal and meridional winds over the high latitude station Andenes (69.3° N, 16.0° E) are found to have significant differences from event to event. Mean wind reversals in the high latitude MLT are found to be preceding the corresponding signatures at 60° N, 10 hPa by a few days. Zonal and meridional wind reversals extend to the MLT region over the mid latitude location Socorro (34.1° N, 106.9° W). However, MLT region over the low latitude station Thumba (8.5° N, 77° E) as well as the equatorial station Kototabang (0.2° S, 100.3° E) are found to be having a minimal response as far as mean winds are concerned. Apart from mean winds, planetary wave activity in the MLT region over the observational sites are examined, which show a systematic progression of planetary waves from high to equatorial latitudes during major as well as minor SSW events. To elucidate the origin of the observed planetary waves in the MLT region, the stratospheric winds are analyzed. Results suggest that the observed planetary waves have originated in the high-mid latitude middle atmospheric region. The present study provides observational evidence for secondary planetary wave generation in the high-mid latitude middle atmosphere and their equatorial propagation in the MLT as predicted by previous numerical modelling studies. Significance of the present study lies in employing a network of meteor radar observations to investigate the SSW signatures in the MLT region over high, middle, low and equatorial latitudes, simultaneously.

1 Introduction

Climatological structure of the high latitude wintertime stratosphere is characterized by a strong eastward flow, which is attributed to the polar vortex, and a negative poleward gradient of temperature. During some winters, the stratospheric polar vortex undergoes rapid weakening or disruption owing to the interaction of anomalously strong planetary waves (PWs) propagating from troposphere with the background stratospheric zonal flow (Labitzke 1971; Andrews et al. 1987). These extreme episodes called Sudden Stratospheric Warming (SSW) events result in warming up of the polar stratosphere by a few tens of degrees of Kelvin, which in turn results in the reversal of the poleward temperature gradient. In some occasions, the zonal wind reverses from eastward to westward direction. It is now known that quasi-stationary planetary waves from the troposphere, predominantly having zonal wavenumbers 1 and 2, interact with the eastward winds in the stratosphere (Matsuno 1971; Holton 1980) and transfer their energy and momentum to the background flow during wave breaking processes, which leads to the warming and wind reversal. Studies on historical records of stratospheric data reveal that such warmings form a climatological feature of the high latitude winter time

✉ N. Koushik
koushiknk@gmail.com

[1] Space Physics Laboratory, Vikram Sarabhai Space Centre, Thiruvananthapuram 695022, India

[2] Savitribhai Phule Pune University, Pune, India

[3] University of Western Ontario, London, Canada

[4] Leibniz Institute of Atmospheric Physics at the Rostock University, Kühlungsborn, Germany

boreal stratosphere (Schoeberl 1978). Owing to the relatively weak polar vortex over the Arctic as compared to that over the Antarctic, SSWs are more common over the former. As planetary wave activity in the winter hemisphere shows significant inter-annual variability and that their interactions with the background flow happen in complex ways, each SSW event is observed to be dynamically unique. Although a universal definition for SSW does not exist (Butler et al. 2015), the most widely accepted one, followed by World Meteorological Organization (WMO), classifies SSWs into major and minor ones. Events which involve a reversal of zonal mean zonal wind at 60° N/S, 10 hPa along with a reversal of zonal mean temperature gradient poleward of 60° N/S, 10 hPa are termed major, and those which do not involve a reversal of zonal mean winds are termed minor SSWs. The polar vortex can be either displaced off the pole or can be completely split into two (Charlton and Polvani 2007) depending on whether the planetary wave involved is of wave number 1 or 2. Accordingly, SSW events are also classified as displacement type and split type SSWs.

Observational as well as numerical modeling studies have confirmed that wind reversal due to planetary wave interaction initially starts deep in the mesosphere over high latitudes, forming a critical layer near the zero wind line. This critical layer further descends with time reaching stratospheric heights where they produce drastic adiabatic warming around the 10 hPa level (Holton 1980). Following SSW events, westward winds in the winter polar stratosphere allow more eastward gravity waves to propagate upward (Liu and Roble 2002). These upward transmitted gravity waves provide substantial eastward forcing in the MLT region, thus reversing the prevailing winds. Using MF and meteor wind radar observations from Northern Hemispheric locations, Hoffmann et al. (2007) observed that strength of wind reversal in the mesosphere in association with SSW events diminishes from high to mid-latitudes. MLT winds were found to reverse, coincident with warming in the high latitude stratosphere as observed by the MF radars at the mid-latitude sites Wuhan (30° N, 114° E) and Langfang (39.4° N, 116.6° E) by Chen et al. (2012). Reversal of MLT winds at the mid latitude location Fort Collins (41° N, 105° W) was found to be linked with a disturbance originating from polar regions during the SSW event of 2009 (Yuan et al. 2012). In a modeling study, Chandran and Collins (2014) observed that there is a warming in the 60–90 km height region above midlatitudes whereas there is a cooling below 60 km. It was also noticed that there is a westward acceleration of the zonal flow and a deceleration of the pole to pole flow in the midlatitude middle atmosphere. Using observations from a chain of eight SuperDARN radars at high latitudes, Stray et al. (2015) investigated the planetary wave response in the MLT region during SSW events. The authors noted that wavenumber 1 and 2 planetary waves enhanced approximately 5 days following wind reversals at 50 km and the enhancements were observed irrespective of the strength of the wind reversal in the high latitude stratosphere. Limpasuvan et al. (2016) emphasized the role played by PW in the MLT region in the formation of elevated stratopause following SSW events as seen in the specified dynamics version of the Whole Atmosphere Community Climate Model (SD-WACCM). It was elucidated that the westward propagating PWs with wavenumber 1, originated from the regions of easterly mean flow in the mesosphere resulting from SSW events.

Over low latitudes, reversal of background zonal and meridional MLT winds during SSW events is not very dramatic. Kishore Kumar et al. (2014) reported the influence of SSW events on the low latitude MLT winds. Most consistently noted feature is the enhancement of semidiurnal tides/oscillations (Pedatella and Forbes 2010; Paulino et al. 2012; Sathishkumar and Sridharan 2013; Koushik et al. 2018). High frequency planetary waves such as quasi 2-day waves were also found to enhance during boreal winters with SSW events (Lima et al. 2012; Koushik et al. 2018). Since winds in the low latitude MLT region significantly influence the ionosphere by means of dynamo mechanism, manifestations of SSW events in low latitude ionosphere are multifarious [For example modulation of equatorial electrojet (Sathishkumar and Sridharan 2013; Siddiqui et al. 2015, 2018), equatorial counter electrojet (Vineeth et al. 2009), variations in total electron content (Yadav et al. 2017; Goncharenko et al. 2018) etc. Refer Chau et al. (2012) for a detailed review]. In addition, several studies demonstrated significant variabilities in planetary and gravity wave activities in the low latitude MLT region during SSW events (Sathishkumar and Sridharan 2009). The interaction of these planetary waves in the MLT with tidal winds is found to be affecting the low latitude ionosphere system (Vineeth et al. 2009).

The propagation of PWs originating from high-mid latitudes during SSW events into the low latitude stratosphere was found to be dependent on the phase of the stratospheric Quasi Biennial Oscillation (QBO) as reported by Chandran and Collins (2014). In another study using WACCM, Chandran et al. (2013) identified secondary planetary waves being generated from high latitude mesosphere- lower thermosphere region following the minor warming event of January 2012. In their study, it was suggested that the baroclinic/barotropic instability of the background zonal flow was responsible for the generation of secondary planetary waves. Using the extended version of SD-WACCM, Sassi and Liu (2014) noticed cross equatorial propagation of westward propagating planetary waves during and after the occurrence of an SSW event. Further, these authors have shown that predominantly upward propagating planetary wave activity, with periods ranging from 2 to 10 days, acquired an equatorward component only

following substantial stratospheric disturbances such as SSWs. In another study using SD-WACCM, Limpasuvan et al. (2016) predicted the generation of 5–12 day PW in the high latitude MLT following major SSW events with elevated stratopause. Using a set of different observations, planetary waves corresponding to wavenumber 1 were noted to enhance in the low latitude mesospheric temperatures by Shepherd et al. (2007). PW generation by jet instabilities in the middle atmosphere has been demonstrated by several studies (Plumb 1983; Hartmann 1983; Tomikawa et al. 2012). Secondary planetary wave generation in the high latitude mesosphere/MLT following SSW events was attributed to the baroclinic/barotropic instability resulting from the reversal of the stratospheric eastward winds by Chandran et al (2013). The authors classify waves observed in the middle atmosphere following the minor SSW of 2012 as long (period > 20 days), medium (period between 10 to 20 days) and short (period < 10 days) period waves.

From the above discussion, it is evident that the dynamics of the MLT region over high, mid and low latitudes are significantly altered during SSW events. It follows from these studies that only a few of them explore the planetary wave activity simultaneously from high to equatorial latitudes in the MLT region following SSW events. In the present study, the mean winds and planetary wave activity in the MLT region using meteor radar observations from four locations representing high, middle, low and equatorial latitudes are investigated. The objective of the study is to analyze the variability of planetary wave activity in the respective MLT regions in response to SSW events and to discuss the possible source mechanism for the observed wave activity. The paper is organized as follows: Sect. 2 describes the meteor wind radar systems, data and analysis techniques used for the study. Discussion on climatological mean winds over the observation location precedes the observations of mean winds and planetary waves during SSW winters in Sect. 3. Section 4 discusses the possible source mechanism for the observations shown in Sect. 3. Concluding remarks are provided in Sect. 5.

2 Data and methods

Meteor wind radar observations from four locations: Andenes (69.3° N, 16.0° E), Socorro (34.1° N, 106.9° W), Thumba (8.5° N, 77° E) and Kototabang (0.2° S, 100.3° E) are used as primary data for the present study. Figure 1 denotes the geographical locations of the radar sites. The four meteor wind radars operate at frequencies 32.55 MHz (peak power 12 kW), 35.24 MHz (peak power 6 kW), 35.25 MHz (peak power 40 kW) and 37.7 MHz (peak power 12 kW), respectively. These multichannel coherent receiver pulsed radar systems are commercially known as all-SKY

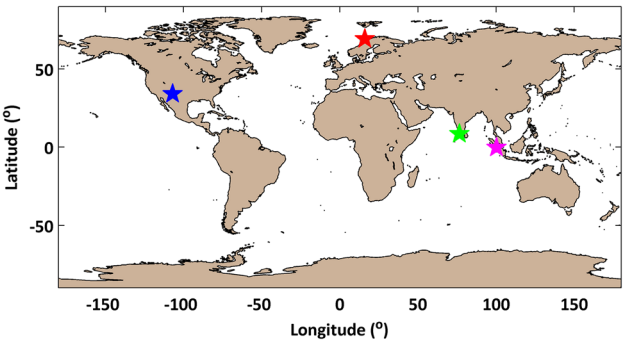

Fig.1 Geographical locations of meteor radars employed for the study: (red) Andenes, (blue) Socorro, (green) Thumba and (magenta) Kototabang

interferometric METeor (SKiYMET) radars. Details of the meteor detection algorithm and wind retrieval can be found in Hocking et al. (2001). Meteor radars at Andenes, Socorro and Thumba provide hourly zonal and meridional winds in the 82–98 km height region in 6 height bins, whereas the system at Kototabang has a vertical resolution of 2 km between 80 and 100 km. Monthly mean climatologies of zonal and meridional winds over the observation locations were constructed using the data spanning from Sep 2001 to Aug 2012, Dec 2008 to Apr 2012, Jun 2004 to Dec 2015 and Jan 2003 to Dec 2012, respectively. Data corresponding to the SSW periods are not excluded while constructing the climatologies, as they have negligible effects in the monthly means. For the present study, MLT observations during three SSW winters viz. 2008–09, 2009–10 and 2011–12 are utilized.

Stratospheric wind, temperature and planetary wave amplitude data used to describe the types of SSW events were obtained from the NASA online data service (https://acd-ext.gsfc.nasa.gov/Data_services/met/ann_data.html). Products in this data service are derived from Modern Era Retrospective Reanalysis for Research and Applications (MERRA) data. Major and minor SSW events were identified using the WMO definition. Central date of the SSW was chosen as the day of wind reversal at 60° N, 10 hPa. In case of the minor SSW of 2011–12, the day of maximum temperature gradient poleward of 60° N, 10 hPa was chosen as the central date. Analyses of stratospheric winds were carried out using the data obtained from European Centre for Medium-Range Weather Forecasts ERA-Interim datasets. Data archived at a horizontal resolution of 1.5° × 1.5° was downloaded from https://www.ecmwf.int/research/era/do/get/index. Details of the ERA-Interim datasets including input data, model used and data assimilation methods involved are outlined in Dee et al. (2011).

Wavelet analysis technique is used to identify planetary wave signatures in the MLT region. This is a well-established

technique and is frequently being used especially to analyze time evolution of the frequency spectrum. More details of the wavelet technique can be found at Torrence and Compo (1998). For the present study, daily mean zonal winds at 88 km are subjected to wavelet analysis to identify planetary wave amplitudes. By making use of daily means, the contributions from semidiurnal oscillations are effectively filtered out.

3 Results

3.1 Climatology of mean winds over the observational sites

Monthly mean climatology of zonal and meridional winds in the MLT region over the observational sites are calculated using long term observations. Figure 2 shows the climatology of zonal winds over the sites (a) Andenes, (b) Socorro, (c) Thumba and (d) Kototabang in terms of height-month sections. Black contours represent zero wind lines. It can be seen that over Andenes (Fig. 2a), the mean zonal wind is characterized by a weak eastward flow during winter at all heights. During summer months (June–August) the zonal flow is strongly westward below 90 km. The summer westward winds gradually decelerate with the onset of autumn, with eastward winds replacing westward winds starting from September. It can be noted that there is a strong eastward jet near the mesopause region (> 90 km) during the summer months. This eastward jet in the MLT can be attributed to the eastward forcing provided by gravity waves propagating upwards through the westward winds below this altitude. Zonal winds over the midlatitude location Socorro (Fig. 2b) also show a strong eastward flow

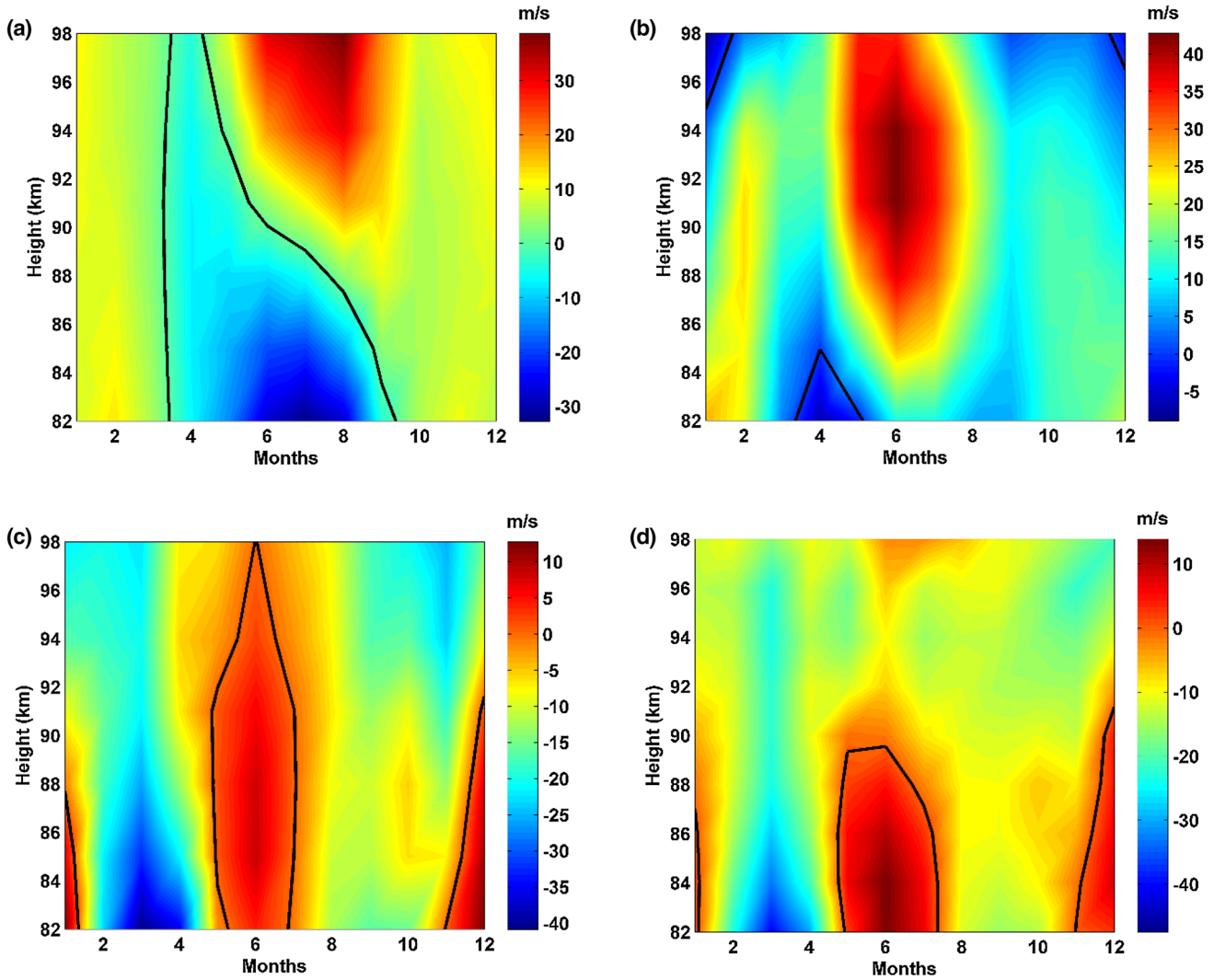

Fig. 2 Monthly mean zonal winds in the MLT region over **a** Andenes, **b** Socorro, **c** Thumba and **d** Kototabang derived from meteor wind radar observations

reaching maximum monthly mean values of around 40 m/s in the 86–98 km height region during summer months. Weak westward winds prevail below 86 km from March to May and above 94 km during December-January months. Over the low latitude and equatorial stations Thumba (Fig. 2c) and Kototabang (Fig. 2d) zonal winds show a strong semiannual oscillation primarily below 90 km and an annual cycle in the 90–100 km height region. Zonal winds are eastward during summer and winter whereas they are westward during the equinoxes. Above 94 km it can be seen that the annual cycle is prevalent, predominantly over Thumba, with eastward winds during May–July months and westward winds otherwise. The semiannual oscillation in the equatorial and low latitude MLT region is a well-known feature driven by the wave-mean flow interactions contributed by gravity as well as equatorial waves (Antonita et al. 2008). It can be summarized that annual cycle is prevalent over the high and midlatitude locations in the entire 80–100 km altitude region, whereas semiannual oscillation in the 80–90 km and annual oscillations above 90 km are present over the low and equatorial latitude stations.

Figure 3 depicts the mean annual cycle of meridional winds over the observational sites in terms of their height-month sections. Over the high latitude station Andenes (Fig. 3a) meridional winds exhibit an annual cycle with the poleward flow during winter months and equatorward flow during summer months. The equatorward flow is found to be stronger than the poleward flow. Figure 3b shows the climatology of meridional winds over the midlatitude site, Socorro. A very clear and strong annual oscillation can be seen in Fig. 3b with the poleward flow during winter months and equatorward flow during summer months. The poleward flow is stronger over Socorro compared to that over Andenes. The annual cycle can be evidently

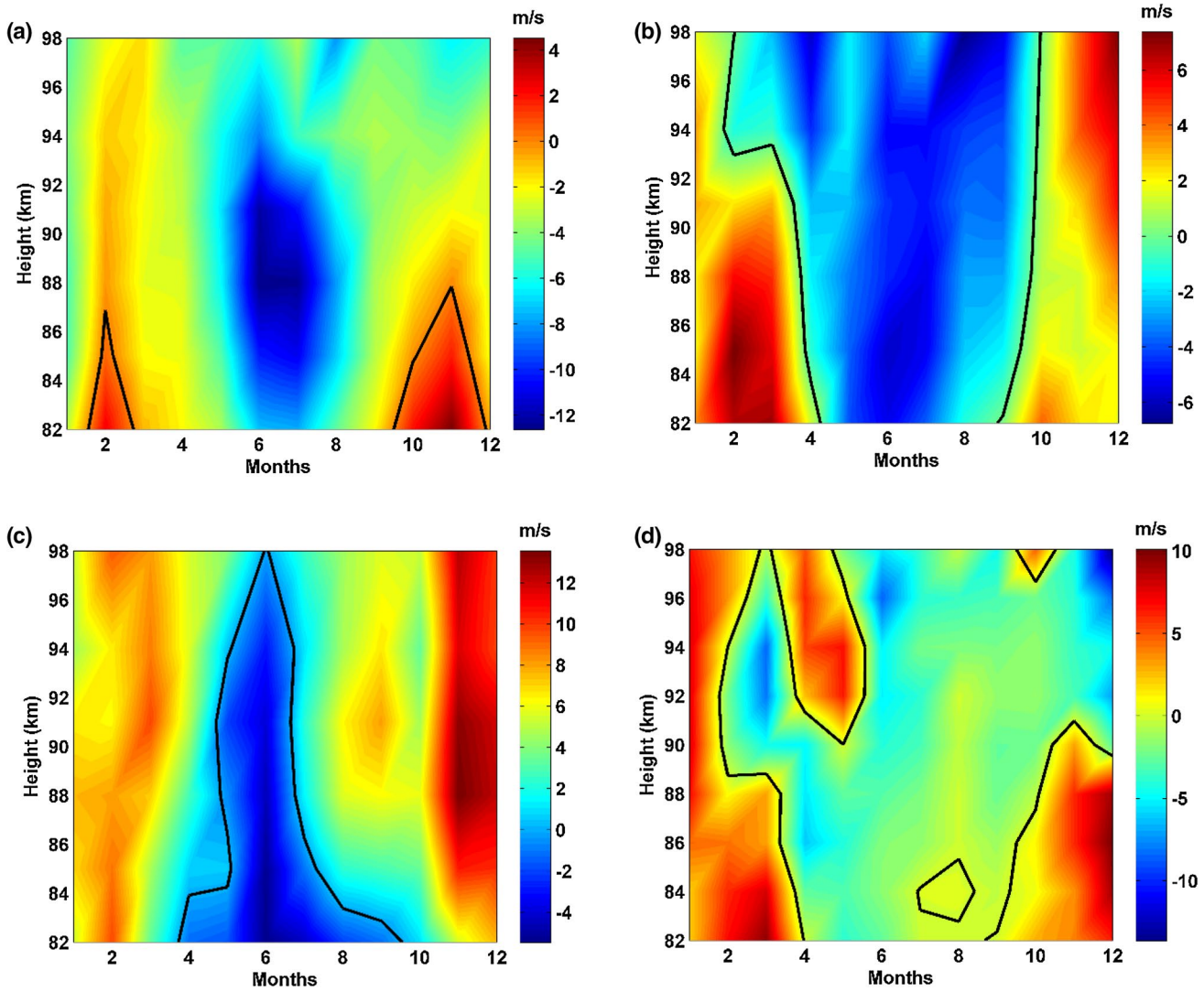

Fig. 3 Same as Fig. 2 but for meridional winds

seen in the meridional wind climatology over the low and equatorial latitude stations Thumba (Fig. 3c) and Kototabang (Fig. 3d), except that southward winds persist in the 90–98 km over Kototabang during October-December months. Poleward (equatorward) winds are stronger (weaker) over the low latitudes than that over high and midlatitudes. It can be seen that the annual climatological cycle in the meridional winds is in accordance with the current understanding of residual circulation in the middle atmosphere. With a pole to pole circulation existing near the mesopause region, winds are poleward during the winter period and are equatorward during the summer period in the northern hemisphere. More discussions on climatologies of mean winds in the MLT region over high, middle and low latitude MLT region can be found elsewhere (Portnyagin et al. 2004; Yuan et al. 2008; Kishore Kumar and Hocking 2010; Ramkumar and Babu 2016; Koushik et al. 2018; Kumar et al. 2018).

3.2 SSW signatures in MLT mean winds

Before discussing the signatures of SSW events in the MLT region, a brief overview of the events under consideration is presented. Figure 4a, b, c illustrate the state of the high latitude stratosphere during 2008–09, 2009–10 and 2011–12 winters, respectively. Top and middle panels show the zonal mean temperature difference between 60 and 90°N and zonal mean zonal wind at 60° N at 10 hPa level, respectively. Amplitudes of planetary waves with zonal wavenumber 1 and 2 are depicted in the bottom panel. Dashed vertical lines indicate the central day of SSW which is defined as the day of wind reversal at 60° N, 10 hPa in case of a major SSW or the day of peak warming poleward of 60° N, 10 hPa in case of a minor SSW. The central days of the SSW events thus identified for the present study are at 55 (24 Jan 2008), 40 (09 Feb 2010) and 49 (18 January 2012). The data period considered spans from 01 December to 28 February of the

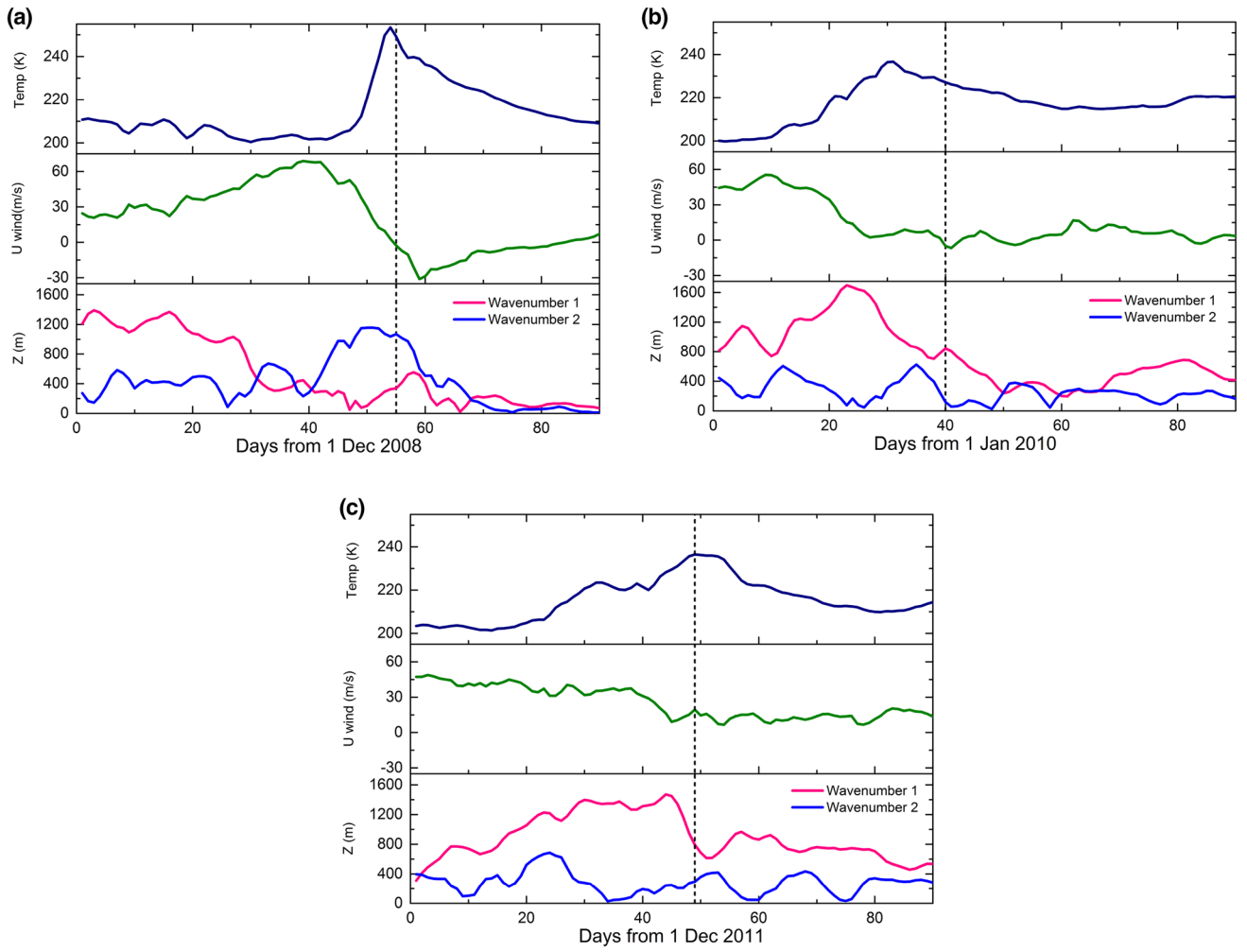

Fig. 4 Temperature at10 hPa averaged between 60–90° N latitude (top panels), zonal mean zonal wind at 60° N, 10 hPa (middle panels) and amplitude of planetary waves with zonal wave number 1 and 2 at 60° N, 10 hPa (bottom panels) for the **a** 2008–09, **b** 2009–10 and **c** 2011–12 events obtained from MERRA datasets

following year. To facilitate a better description, the data period considered for the 2009–10 winter spans from 01 January to 31 March since the SSW happened in the month of February. It can be seen that in all the three cases, the increase of temperature in the polar cap is almost coincident with the deceleration of zonal wind at 60° N. Wavenumber 1 is the dominant component in 2009–10 and 2011–12 winters, whereas 2008–09 winter shows the dominance of wavenumber 2 resulting in a split type SSW. The 2008–09 SSW is exceptional in terms of the resultant temperature difference and also in terms of strength and duration of the wind reversal.

Figure 5 depicts the height-time sections of the zonal winds in the 82–98 km height region over the observational sites. Each panel represents observations over four sites for a given SSW event. Wind observations over Kototabang for the 2009–10 period is not considered as there were significant data gaps during the period. Vertical solid black lines indicate the central day of the SSW. White regions indicate data gaps. It can be seen from Fig. 5a that the zonal wind over the high latitude site Andenes reversed 4–5 days before the onset of the SSW. Westward winds replace eastward winds around the central day and a strong eastward flow remains afterward. During the wind reversal, westward winds reach amplitudes ~ 40 m/s. Reversal of mean zonal winds from eastward to the westward in the MLT region over the midlatitude site Socorro is almost coincident with the central day of the SSW as can be seen in Fig. 5b. An even stronger reversal can be seen penetrating from above, persisting up to day 65. Strong eastward winds prevail after the reversal dissipates. Over the low and equatorial latitude stations Thumba and Kototabang, no SSW induced wind reversal is visible (Fig. 5c, d) as a reversal of mean zonal wind persists as a part of the climatological seasonal change over both the sites (see Fig. 2c, d). For the 2009–10 SSW event, it can be seen from Fig. 5e that there is no significant change in the mean zonal winds over Andenes. Zonal winds over Socorro (Fig. 5f) reverse almost 10 days before the wind reversal in high latitude stratosphere and eastward winds prevail during the warming. Though a patch of westward winds shows up over Thumba (Fig. 5g), it seems that these winds are associated with planetary wave perturbations as they appear periodically. For the minor SSW event of January 2012, winds in the high latitude MLT slightly decelerate before the central day (Fig. 5h). It can be seen from Fig. 5i that the zonal wind reversal persists to several days after the central day over Socorro and eastward winds prevail after the reversal subsides. Figure 5j, k reveal stronger patches of westward winds reaching from above up to 85 km over Thumba and up to 88 km over Kototabang. Whether these observed changes in zonal winds over Thumba and Kototabang are associated with minor SSW or not is yet to be ascertained as other westward wind bursts can also be observed away from the central day. However,

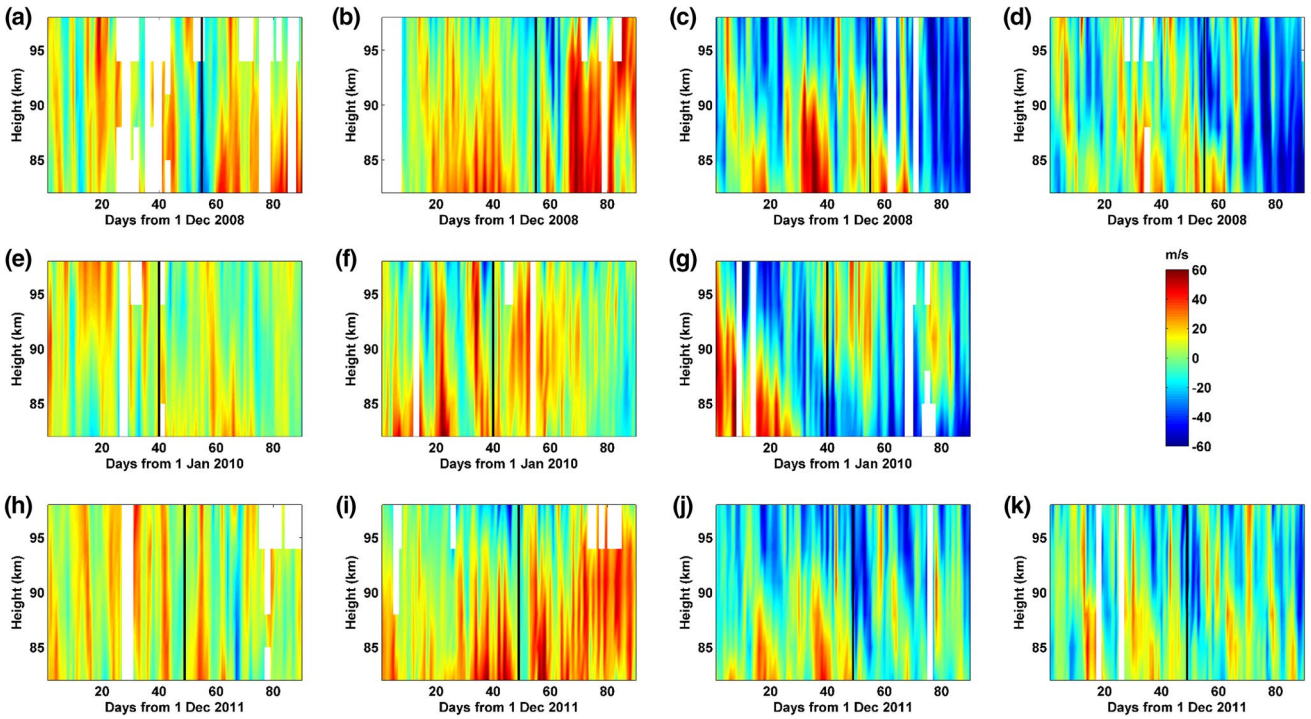

Fig. 5 Height-date sections of meteor radar derived MLT zonal winds during (top) 2008–09, (middle) 2009–10 and (bottom) 2011–12 events over the observational sites **a**, **e**, **h** Andenes, **b**, **f**, **i** Socorro, **c**, **g**, **j** Thumba and **d**, **k** Kototabang

the observed westward winds over these latitudes around the central day are relatively stronger as compared to other days. A closer examination of Fig. 5a, e, h suggest that zonal wind signatures of SSW events in the high latitude MLT vary from event to event. This can be attributed to the zonal asymmetry associated with the SSW events. Since planetary waves themselves imply a deviation from zonal symmetry, the wind reversals resulting from their interactions with the background zonal winds are also expected to have a non-zonal behavior. Also, the location of the observational site with respect to the final warming also may have implications in the observed features in the MLT region. Zonal wind reversals during SSW winters are found to extend up to the midlatitude MLT region, however the time of occurrence of wind reversal can vary significantly from the central day identified by the WMO definition. The low and equatorial latitude MLT region does not show a significant (distinct) zonal mean wind response to SSW events.

Figure 6 shows the height-time sections of meridional winds in the 82–98 km height region for the three SSW events considered. Meridional winds over the high latitude site Andenes exhibit strong equatorward flow before the central day of the 2008–09 SSW event, followed by intense poleward flow during the warming period as shown in Fig. 6a. The poleward flow lasts for approximately 5 days with peak value almost 50 m/s. Figure 6b shows the meridional wind evolution for the same SSW event over Socorro. It can be seen that strong equatorward flow immediately follows the central day. Thereafter meridional winds abruptly become poleward before returning to normal values. Over the low and equatorial latitude sites Thumba (Fig. 6c) and Kototabang (Fig. 6d) no significant reversal of meridional winds is evident. But it can be seen that short term fluctuations in the meridional winds amplify near to the central day of SSW. For the major SSW event of 2009–10, the meridional wind over Andenes (Fig. 6e) is seen to become poleward ~ 10 days before the wind reversal at 60° N, 10 hPa. Moderately strong equatorward flow persists just before the central day of the SSW at day 40. No significant wind reversal can be seen over Socorro (Fig. 6f) for the February 2010 event but it can be observed that wavy structures start to appear well before the central day, starting from day 30. Same as the 2008–09 event, for the 2009–10 event also very short term fluctuations become prominent over Thumba (Fig. 6g). From Fig. 6h it can be understood that strong equatorward flow starting from day 30 persists up to the central day for MLT region over Andenes for the 2011–12 case. Thereafter poleward flow takes over again. Over Socorro, short term fluctuations become evident after the central day (Fig. 6i). Again, over the low latitude station, Thumba (Fig. 6j) and equatorial station Kototabang (Fig. 6k) short term disturbances show up around the central day of the minor SSW. From the meridional wind observations in the high latitude MLT during SSW winters, it can be seen that the meridional flow largely depends on the location of the split/displaced vortex. The climatological circulation in the high latitude

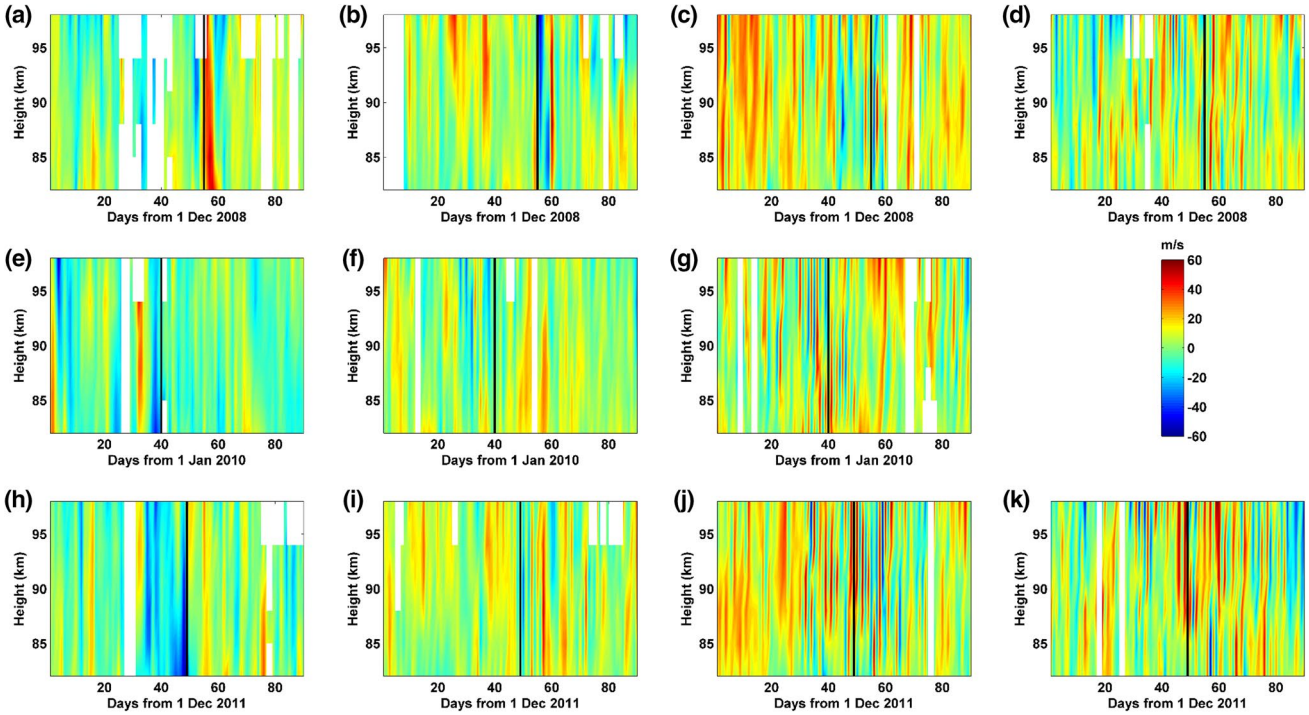

Fig. 6 Same as Fig. 5 but for meridional winds

MLT consists of a summer to winter pole circulation. Hence during quiet wintertime conditions high latitude MLT region exhibits a poleward flow. During an SSW episode, after the reversal of winds in the stratosphere, due to the breaking of eastward propagating gravity waves, there is a resultant adiabatic upwelling and cooling which offsets the existing temperature gradient. Accordingly, we expect an equatorward flow to happen in the high latitude MLT region. However, for the 2008–09 SSW event meridional winds over Andenes show a strong poleward flow. This is because at the time of the 2008–09 SSW, the anticyclone is present equatorward of Andenes above which MLT upwelling occurs (Chandran and Collins 2014). In the other two cases, it can be observed that the meridional flow becomes equatorward in the high latitude MLT around the time of SSW. A general tendency of midlatitude MLT region is to show enhanced equatorward flow in connection with SSW events. This is most likely resulting from the temperature offset created by high latitude MLT cooling during SSW events. Meridional winds over the low and equatorial stations Thumba and Kototabang consistently show very short term fluctuations during SSW events. This is because of the enhancement of quasi 2-day wave amplitudes resulting from SSW events (McCormack et al. 2009; Lima et al. 2012; Gu et al. 2016; Koushik et al. 2018). In all the three winters considered in the study, this feature is markedly seen.

3.3 SSW signatures in MLT planetary waves and their relation to the underlying stratosphere

The planetary wave activity in the MLT region during SSW winters is analyzed over the four observational sites. For this purpose zonal winds at 88 km altitude obtained from meteor radar observations are used. The wavelet analysis technique is employed to identify the time evolution of planetary wave periodicities in the MLT region. 'Morlet' wavelet is chosen as the mother wavelet. Upper panels of Figs. 7, 8, 9 denote the wavelet spectra of zonal winds at 88 km over the observation locations. Data gaps if any are linearly interpolated before subjecting to wavelet analysis. Vertical dotted lines denote the central days of the SSWs. Slanted lines represent the cone of influence which is the region beyond which edge effects become prominent. White contours indicate 95% confidence level for wavelet amplitudes. Since planetary wave activity in the MLT is largely dependent on the winds and waves in the underlying atmosphere, an attempt is made to link them to winds in the 100–1 hPa height region (middle

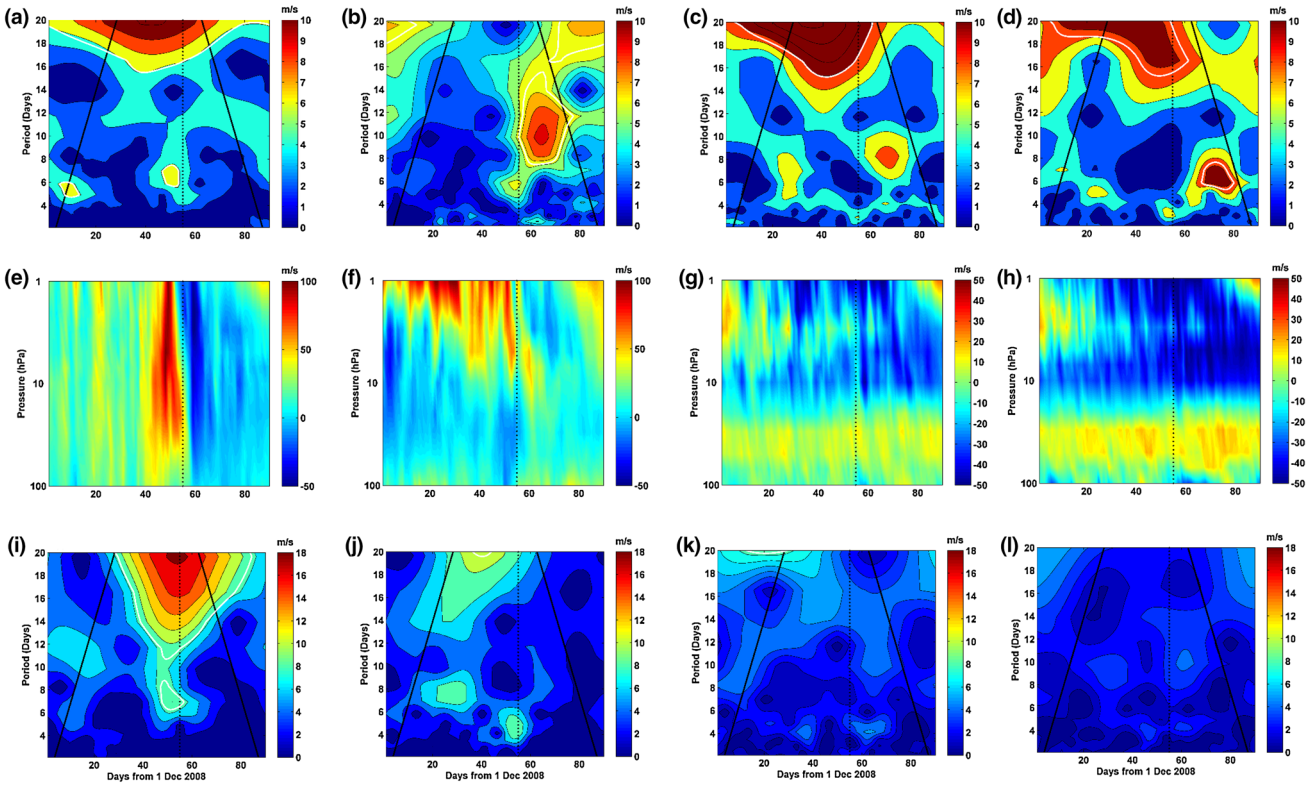

Fig. 7 Wavelet spectra of meteor radar derived zonal winds at 88 km over **a** Andenes, **b** Socorro, **c** Thumba and **d** Kototabang, the corresponding stratospheric winds over **e** Andenes, **f** Socorro, **g** Thumba and **h** Kototabang from ERA-interim datasets, and wavelet spectra of zonal winds at 1 hPa over **i** Andenes, **j** Socorro, **k** Thumba and **l** Kototabang for 2008–09 winter from ERA-interim datasets

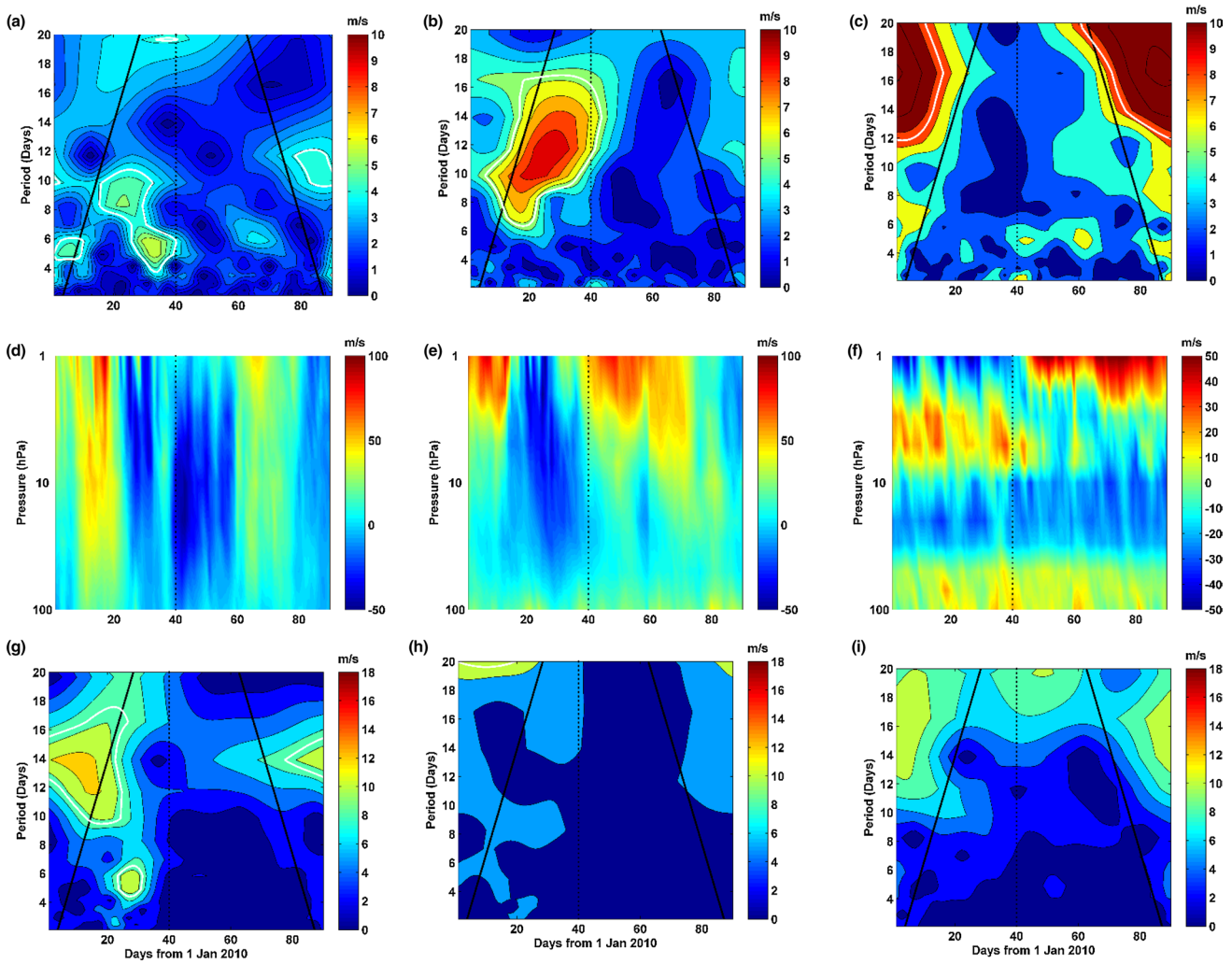

Fig. 8 Wavelet spectra of meteor radar derived zonal winds at 88 km over **a** Andenes, **b** Socorro and **c** Thumba, corresponding stratospheric winds over **d** Andenes, **e** Socorro and **f** Thumba from ERA-interim datasets and wavelet analysis of zonal winds at 1 hPa over **g** Andenes, **h** Socorro and **l** Thumba for 2009–10 winter from ERA-interim datasets

panels) and to the planetary wave activity at 1 hPa (bottom panels

Figure 7e–h depicts the zonal winds in the 100–1 hPa pressure levels over the nearest geographical locations of four observational sites obtained from ERA-Interim Reanalysis Dataset during the 2008–09 winter. Bottom panel gives the wavelet spectrum of zonal winds at 1 hPa. The primary focus will be on planetary wave periodicities < 20 days since periodicities > 20 days are often classified as quasi stationary waves and are found to be primarily responsible for the generation of SSWs (Matsuno 1971). From Fig. 7a it can be seen that there are enhancements of wavelet amplitudes near 4–6 day periodicities close to day 10 and 6–8 day periodicities close to day 50 over the high latitude location Andenes. A portion of the former peak happens to be outside the cone of influence and hence is not considered to be reliable. A ~ 20 day period wave also can be noted from this figure before the central day. Winds in the underlying stratosphere start reversing at 1 hPa a few days before the central day and rapidly propagate downwards (Fig. 7e). At the same time at 1 hPa, ~ 20 day and ~ 6–8 day periodicities enhance near the central day (Fig. 7i). Interestingly, the PW with period 6–8 days is not observed at 10 hPa (figure not shown). From Fig. 7b it is evident that there are two distinct peaks in wavelet amplitudes at 88 km over Socorro, one with 4–6 day periodicity almost coinciding with the wind reversal and another one with ~ 10 day periodicity peaking around day 65, approximately 10 days after the central day. Winds in the underlying stratosphere reverse after the central day persisting up to day 75 (Fig. 7f). A 4–6 day period wave is also found to be enhanced at 1 hPa around the day of wind reversal (Fig. 7j). On closer examination, it can be identified that the 4–6 day periodicity appears to propagate from the stratopause region whereas the ~ 10 day periodicity is

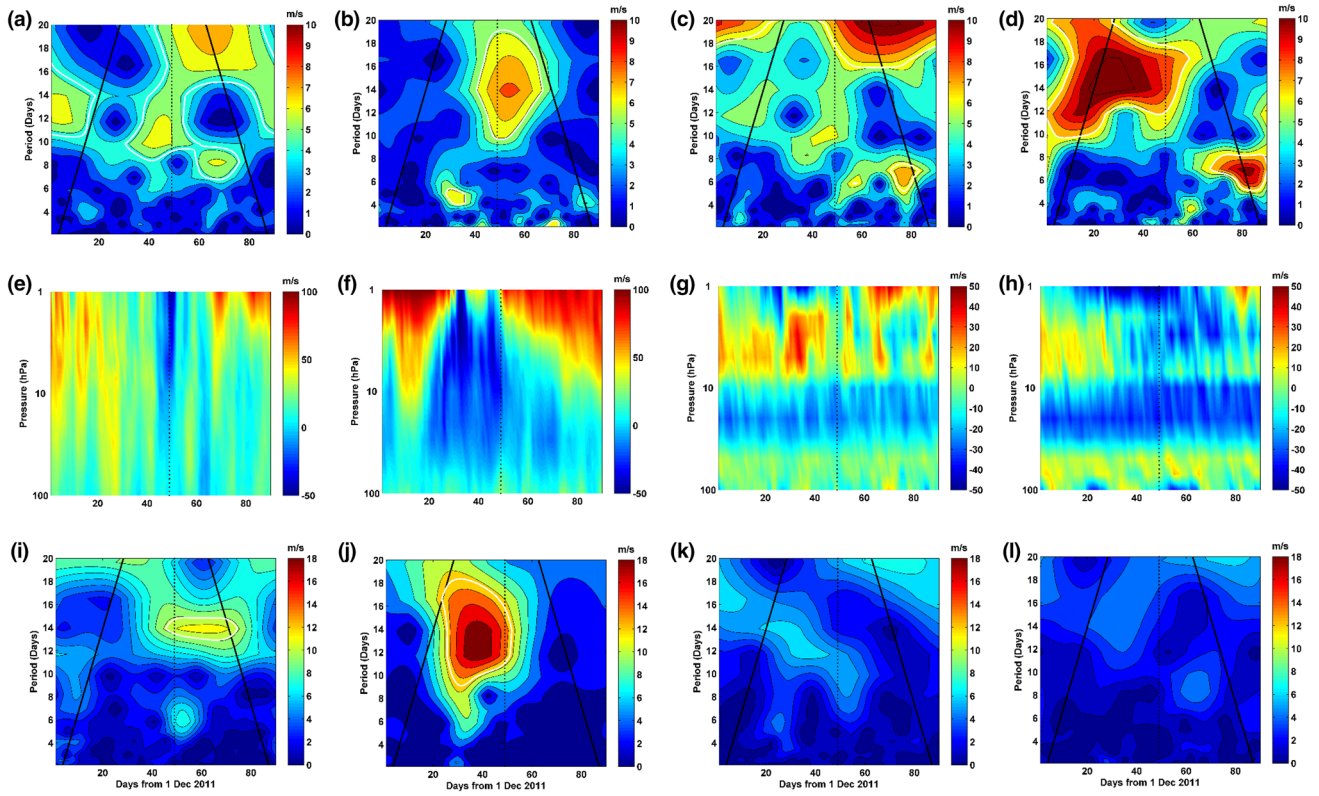

Fig. 9 Same as Fig. 7 but for 2011–12 winter

not present in the stratosphere. There were no signatures of PW with these periods at 10 hPa level. Over low and equatorial latitude stations Thumba (Fig. 7c) and Kototabang (Fig. 7d), 6–10 day periodicities enhance after the central day. It should be noted that there is a marked time delay in the occurrence of the peaks over these two locations compared to that over Socorro as seen in Fig. 7b. Also, there is a slight time delay between the occurrence of the peaks over Thumba and Kototabang. However, it has to be noted that the peak observed over Thumba does not fall under the 95% significant region. It is seen that this peak over Thumba is above the 90% significance level (not shown). There is even a slight difference in the central time period of this wave over the three locations. Over Socorro, the observed time period is centered on ~ 10 day, it is ~ 8 day over Thumba and ~ 6 days over Kototabang. However, overall the observed time period is in the range of 6–10 days. The underlying stratospheric region over Thumba and Kototabang (Fig. 7g, h) does not exhibit any wind reversals in connection with the SSW event. Also there are no statistically significant PW periodicities observed at 1 hPa (Fig. 7k, l). It follows from these features that the enhancements observed over Thumba and Kototabang are not propagating from below.

For the 2009–10 winter, wavelet spectra at 88 km over Andenes, Socorro and Thumba are depicted in Fig. 8a, b, c, respectively. Over the high latitude site Andenes enhancement of 8–10 day and 4–6 day periodicities can be observed around day 25 and 35, respectively. Winds in the 100–1 hPa region over Andenes reverse well in advance of the central day, starting from around day 25 (Fig. 8d). The wind reversal persists up to day 60 before turning eastward. In the 1 hPa region, enhancement of 4–6 day periodicity can be observed near to day 25 (Fig. 8g). Though winds in the underlying stratosphere stay reversed (Fig. 8e) during the enhancement of ~ 12 day periodicity at 88 km (Fig. 8b), no statistically significant periodicity is observed in the 1 hPa level (Fig. 8h) over Socorro. Over Thumba, two blobs of enhancements can be seen after the central day at 88 km (Fig. 8c), though they are not significant at the 95% confidence level. During this period there is no abrupt reversal of zonal winds in the underlying stratosphere (Fig. 8f) and no presence of significant waves at 1 hPa (Fig. 8i). Above discussions suggest that PW enhancement seen in the MLT over Andenes generally seems to propagate from below, whereas enhancements over Socorro and Thumba are not related to the underlying atmosphere in a similar sense.

Figure 9a shows the wavelet spectra of zonal wind at 88 km over Andenes during the minor SSW winter 2011–12. There are two statistically significant enhancements corresponding to ~ 10 day and ~ 8 days appearing immediately

before the central day and ~ 15 days after the central day. Stronger wind reversals near to 1 hPa get diluted on reaching lower altitudes, lasting from around days 40 to 65 (Fig. 9e). Significant enhancement in planetary wave activity with ~ 14 day periodicity is observed at 1 hPa after the central day (Fig. 9i) over Andenes. Over Socorro at 88 km (Fig. 9b), enhancements are seen for 4–6 day periodicity during 30–40 days and for a broader peak centered at ~ 14 days after the central day. Winds in the 100–1 hPa region (Fig. 9f) reverse (two significant reversals at 1 hPa) coinciding with the broader enhancement of PW periodicities at 1 hPa, peaking at 12–14 days (Fig. 9j). Interestingly, the 12–14 day PW observed at 1 hPa was completely absent at 10 hPa (figure not shown) thus emphasizing the origin of the observed PW at stratopause region. Even though no statistically significant PW periodicity at 1 hPa (Fig. 9k, l) or abrupt wind reversals at 100–1 hPa region (Fig. 9g, h) are observed over Thumba and Kototabang, enhancements of 4–8 day periodicities can be seen at 88 km (Fig. 9c, d). Wavelet periodogram at 88 km over Kototabang (Fig. 9d) also shows a statistically significant enhancement of 12–16 day periodicity well before the SSW onset. Observing the above features, it can be inferred that for the minor SSW event of 2011–12, the wind reversal in the stratosphere over the midlatitude station Socorro is stronger than that over the high latitude site Andenes. Similarly, both planetary wave amplitudes at 1 hPa and at 88 km are stronger over Socorro than over Andenes. As mentioned earlier, each event of SSW, whether major or minor, manifests uniquely in the MLT region and following section aimed at discussing some general features and interpreting the results presented in this section.

4 Discussion

On closer examination of Fig. 7a it becomes clear that the PW enhancements seen in the MLT over Andenes are directly linked to the underlying stratopause region as similar peaks appear in the wavelet spectrum at 1 hPa (Fig. 7i). It is also noted that the observed PW activity at 1 hPa is completely absent at 10 hPa (figure not shown), thus providing an evidence for generation of secondary planetary waves around the stratopause region over the high latitudes. Limpasuvan et al. (2016) suggested that during SSW events, 30–80 km region over high latitudes favors the generation of westward propagating secondary planetary waves through the occurrence of barotropic or baroclinic jet instability. Over Socorro, a broad peak of 8–12 day periodicity at 88 km (Fig. 7b) appears immediately after the central day and is statistically significant. A weaker wind reversal can be observed around the same time starting from 1 hPa (Fig. 7f). However, there is no enhancement in the corresponding periodicity at 1 hPa. This leads us to argue that the 8–12 day PW enhancement seen over Socorro is not propagating from below and hence is generated by other mechanisms. Similar are the situations over Thumba and Kototabang (Fig. 7c, d) where there are no abrupt wind reversals or PW enhancement at 1 hPa. These observations suggest that the PWs observed over Andenes, Socorro, Thumba and Kototabang are secondary planetary waves excited at or above 1 hPa level and propagating from high latitudes towards lower latitudes. Several numerical modeling studies have demonstrated that secondary planetary waves are generated in the mid-high latitudes in the mesosphere or MLT region and that they propagate upward and equatorward (Chandran et al. 2013). Proposed mechanisms behind the generation of secondary planetary waves in the MLT are in-situ generation of PWs by zonally asymmetric gravity wave breaking (Liu and Roble 2002), baroclinic/barotropic instability of the background zonal flow (Chandran et al. 2013), and PW amplification by stimulated tidal decay (PASTIDE, He et al. 2017). Systematic progression of time of occurrence of PW enhancements over mid and low latitudes observed in this study suggests that they are propagating meridionally in the MLT region. It should be noted that there is a finite difference in the periodicity of the waves observed over the middle and low latitude stations. This could arise because of (1) Doppler shift in the frequencies of these traveling waves or (2) broadening of spectral response due to variations in background winds (Salby 1981; Pancheva et al. 2008).

During the 2009–10 SSW event, PW enhancement seen in the MLT over Andenes (Fig. 8a) can be linked to the underlying stratopause since similar PW enhancement can be noted at 1 hPa (Fig. 8g), with the 1 hPa peak leading the peak at 88 km. Over Socorro, PW enhancement in the MLT (Fig. 8b) can be seen coinciding with wind reversal in the underlying 100–1 hPa region (Fig. 8e). After the central day, the PW activity diminishes in the MLT, concurrent with winds turning eastward in the underlying stratosphere. Statistically significant signatures of similar PW periodicities are not observed at 1 hPa. In the MLT region over the low latitude station Thumba also PW enhancement corresponding to 4–6 day period can be observed (Fig. 8c) without any prominent signatures in the underlying stratosphere. The major difference between 2009–10 and 2008–09 events is that PW enhancements in the midlatitude MLT region are observed before the central day in 2009–10 and after the central day in 2008–09.

Contrary to the previous two cases, the planetary waves in the MLT region over the high latitude station Andenes during the minor SSW winter 2011–12 (Fig. 9a) do not seem to be propagating from stratopause region as no statistically significant PW enhancement is observed at 1 hPa level (Fig. 9i) concurrent with PW activity in the MLT prior to the central day. At the same time, 1 hPa level over Socorro shows a very strong and broad PW enhancement centered

at ~ 14 days (Fig. 9j). The PW activity at 10 hPa level (not shown) did not show the signature of ~ 14 day wave thus indicating the stratopause as the source region as discussed earlier. Concurrently, winds in the 100–1 hPa region show strong westward flow (Fig. 9f). A small patch of PW activity lasting for about 10 days starting from day 30 is seen in the MLT region with period 4–6 days over Socorro when winds in the 100–1 hPa region remain reversed. A broader PW enhancement can also be seen at 88 km over Socorro after the central day with period 12–14 days. It is observed that at 85 km 12–14 day PW has larger amplitudes than that of 88 km (not shown). The amplitude of the PW was even larger at 82 km. This suggests that either the wave undergoes weakening as it approaches 88 km or it undergoes an equatorward turning at that altitude. It is also worth noting that a similar enhancement in the 12–14 day PW activity can be seen at 1 hPa over Andenes after the central day of the SSW. The observed periodicities fall strikingly similar to the one seen in the midlatitude stratosphere with a finite time delay. It can be seen from the middle panels of Fig. 9 that reversal of zonal winds is stronger and more persistent over Socorro than over Andenes. This indicates that PW amplitudes were also larger over Socorro than over Andenes at 1 hPa level. Hence secondary PW generation is more likely to be resulting from midlatitude middle atmosphere. Similar to the 2008–09 event, PW enhancements corresponding to periodicities 6–8 days appear over Thumba and Kototabang starting from day 60 onwards. These peaks are found to fall well within the statistically significant region. Thus it can be inferred that strong secondary PWs are generated in the midlatitude MLT region following the 2011–12 minor SSW and they propagate equatorward reaching low-equatorial latitudes.

Several aspects of coupling between the high and low latitude middle atmosphere exist in the literature. This coupling is largely attributed to large scale planetary waves prevalent in the winter middle and high latitudes. Planetary wave propagation in to middle and high latitude was found to be modulated by the phase of the equatorial Quasi Biennial Oscillation (Holton and Tan 1980, 1982). Accordingly occurrences of SSW events were also found to have a dependence on the phase of the QBO. However robustness of this 'Holton-Tan' mechanism is still debated over (Anstey and Shepherd 2014). de Wit et al. (2015) discussed the coupling aspects related to the 2013 SSW in the light of interhemispheric coupling mechanism (Becker and Fritts 2006; Karlsson et al. 2009; Körnich and Becker 2010) wherein temperature anomalies in the MLT region over summer high latitudes are attributed to strong planetary wave activity prevailing in the winter stratosphere. Since SSW events form an extreme case for wintertime stratospheric planetary wave activity, it can as well be considered as an example demonstrating the interhemispheric coupling. It should be noted that cross-equatorial propagation of planetary waves has been demonstrated in several numerical modeling studies (Forbes et al. 1995) as well as observations (Riggin et al. 2006; John and Kumar 2016).

Comparison of present results with Chandran et al (2013) suggests that medium period waves are mostly observed over midlatitudes and short period waves are observed over low and equatorial latitudes. Present results are in accordance with Sassi and Liu (2014) in that the periodicities of PWs observed in low latitudes fall in the model predicted 2–10 day range and that we see a systematic temporal progression of wave activity from mid to low latitudes following the three SSW events. Even though we do not present a thorough analysis based on potential vorticity gradient demonstrating regions favorable for instability generation, present observations suggest that significant wind reversals observed in the high and midlatitude stratosphere following SSW events favor the instability mechanism for the generation of secondary planetary waves. However in-situ generation of MLT planetary waves by zonally asymmetric gravity wave breaking (Dunkerton and Butchart 1984; Holton 1984; Smith 1996, 1997; Liu and Roble 2002) cannot be ruled out.

Similar equatorward propagation of planetary waves following SSW events was also established by Chandran and Collins (2014). In their study, propagation of PWs from high to low latitudes in the stratosphere was found to depend on the phase of the stratospheric QBO. The easterly phase of the QBO facilitated cross equatorial propagation of the disturbances. On the other hand, PW propagation terminated at ~ 20–25° N during the westerly counterpart of the QBO. Present results however suggest that such a dependence on phase of the QBO does not exist as far as the PWs observed in the MLT are concerned. It can be noted from Figs. 7, 8, 9 that the phases of the QBO are westerly, easterly and easterly, respectively for the three cases considered. But during all the three cases PW enhancements were observed in the low latitude MLT. This suggests that these PWs propagate horizontally in the MLT region subsequent to their generation in the high-mid latitude middle atmosphere.

5 Concluding remarks

Using meteor wind radar observations at four locations Andenes, Socorro, Thumba and Kototabang representing high, middle, low and equatorial latitudes, respectively, the response of the MLT region to SSW events that occurred during the winters of 2008–09, 2009–10 and 2011–12 are investigated. Climatology of monthly mean winds, variability in mean winds and planetary wave activity in the MLT region over four observational sites during SSW events including a possible mechanism for the observed variability are discussed. Apart from the MLT region wind

observations, stratospheric wind data from ERA-Interim datasets are employed. The following are the main conclusions drawn from the study,

(i) Signatures of SSW events in the MLT region over high latitude zonal and meridional winds are found to have significant variabilities from event to event. This is most likely because of the differences in planetary wave-mean flow interaction and the resultant location of wind reversal in the underlying stratosphere. The mean wind responses in the MLT are found to precede the corresponding signatures in the stratosphere by a few days over high latitudes. Mean winds in the middle latitudes show moderate response to SSW events as compared to high latitudes. Temporal evolution of these signatures is again found to vary from event to event. Low as well as equatorial latitude MLT region is found to have a minimal response as far mean winds are concerned. These observations thus confirm that the signatures of SSW in the MLT region mean winds are confined to high and mid-latitudes.

(ii) Our major emphasis is on investigating the planetary wave activity in the MLT region simultaneously over the four observational sites during SSW events. PW enhancements are observed over high, middle, low and equatorial latitude MLT in association with major as well as minor SSW events. Over high latitudes, these enhancements are often found to lead before the central day of the SSW. Over midlatitudes, PW enhancements are generally stronger than those over high latitudes. Similar PW enhancements are also observed over low and equatorial latitude MLT region. PW enhancements are found to have a systematic temporal progression from high/mid to low latitudes suggesting their equatorward propagation in the MLT region.

(iii) Examination of underlying stratospheric winds and waves suggest that in the high latitude MLT, planetary wave enhancements are often (not always) related to PW activity from the stratopause region (1 hPa). Here it should be remembered that, the stratopause (1 ha) level considered in this study encompasses the region favorable for the generation of secondary planetary waves in high latitudes through shear instabilities resulting from SSW events. Thus presence of similar PW periodicities in high latitude MLT and stratopause need not necessarily imply their tropospheric origin. Further, it is examined that the observed PWs at 1 hPa are absent at 10 hPa level. These observations provide evidence for in-situ generated PW possibly at and above the stratopause level. Over midlatitudes, underlying stratospheric wind reversals are found to play a major role in the observation of PW enhancements. No relation to underlying winds or waves is observed over low and equatorial latitudes.

(iv) These observations suggest that PWs are generated in-situ in the high-mid latitude middle atmosphere and they propagate equatorward in the MLT region. Though efforts are not made in the present study to bring out the mechanism for observed secondary PWs, based on observations from the underlying stratosphere as well as results from earlier numerical studies, it is suggested that the instability of the stratospheric jet and/or in-situ generation of PWs by zonally asymmetric gravity wave breaking could be potential candidates for the generation of secondary planetary waves observed in the MLT. The present observations are in agreement with the previous numerical modeling studies on SSW signatures in the MLT region.

Acknowledgements N. Koushik gratefully acknowledges the financial support and research opportunity provided by Indian Space Research Organisation for his research work. Data acquisition of meteor wind radar at Kototabang has been done by Research Institute for Sustainable Humanosphere (RISH), Kyoto University. Distribution of the data has been partly supported by the IUGONET (Inter-university Upper atmosphere Global Observation NETwork) project (https://www.iugonet.org/) funded by the Ministry of Education, Culture, Sports, Science and Technology (MEXT), Japan. The high latitude stratospheric parameters were obtained from the NASA online data service (https://acd-ext.gsfc.nasa.gov/Data_services/met/ann_data.html). The stratospheric wind data used in this study have been obtained from European Centre for Medium-Range Weather Forecasts ERA-Interim reanalysis (https://www.ecmwf.int/research/era/do/get/index).

References

Andrews DG, Holton JR, Leovy CB (1987) Middle atmosphere dynamics. Academic Press, New York

Anstey JA, Shepherd TG (2014) High-latitude influence of the quasi-biennial oscillation. Q J R Meteorol Soc 140:1–21. https://doi.org/10.1002/qj.2132

Antonita TM, Ramkumar G, Kumar KK, Deepa V (2008) Meteor wind radar observations of gravity wave momentum fluxes and their forcing toward the Mesospheric Semiannual Oscillation. J Geophys Res 113:1–12. https://doi.org/10.1029/2007JD009089

Becker E, Fritts DC (2006) Enhanced gravity-wave activity and interhemispheric coupling during the MaCWAVE/MIDAS northern summer program 2002. Ann Geophys 24:1175–1188. https://doi.org/10.5194/angeo-24-1175-2006

Butler AH, Seidel DJ, Hardiman SC et al (2015) Defining sudden stratospheric warmings. Bull Am Meteorol Soc 96:1913–1928. https://doi.org/10.1175/BAMS-D-13-00173.1

Chandran A, Collins RL (2014) Stratospheric sudden warming effects on winds and temperature in the middle atmosphere at middle and low latitudes: a study using WACCM. Ann Geophys 32:859–874. https://doi.org/10.5194/angeo-32-859-2014

Chandran A, Garcia RR, Collins RL, Chang LC (2013) Secondary planetary waves in the middle and upper atmosphere following the stratospheric sudden warming event of January 2012. Geophys Res Lett 40:1861–1867. https://doi.org/10.1002/grl.50373

Charlton AJ, Polvani LM (2007) A new look at stratospheric sudden warmings. Part I: Climatology and modeling benchmarks. J Clim 20:449–469. https://doi.org/10.1175/JCLI3996.1

Chau JL, Goncharenko LP, Fejer BG, Liu HL (2012) Equatorial and low latitude ionospheric effects during sudden stratospheric warming events: ionospheric effects during SSW events. Space Sci Rev 168:385–417. https://doi.org/10.1007/s11214-011-9797-5

Chen X, Hu X, Xiao C (2012) Variability of MLT winds and waves over mid-latitude during the 2000/2001 and 2009/2010 winter

stratospheric sudden warming. Ann Geophys 30:991–1001. https://doi.org/10.5194/angeo-30-991-2012

De Wit RJ, Hibbins RE, Espy PJ, Hennum EA (2015) Coupling in the middle atmosphere related to the 2013 major sudden stratospheric warming. Ann Geophys 33:309–319. https://doi.org/10.5194/angeo-33-309-2015

Dee DP, Uppala SM, Simmons AJ et al (2011) The ERA-Interim reanalysis: Configuration and performance of the data assimilation system. Q J R Meteorol Soc 137:553–597. https://doi.org/10.1002/qj.828

Dunkerton TJ, Butchart N (1984) Propagation and selective transmission of internal gravity waves in a sudden warming. J Atmos Sci 41:1443–1460. https://doi.org/10.1175/1520-0469(1984)041%3c1443:PASTOI%3e2.0.CO;2

Forbes JM, Hagan ME, Miyahara S et al (1995) Quasi 16-day oscillation in the mesosphere and lower thermosphere. J Geophys Res 100:9149. https://doi.org/10.1029/94JD02157

Goncharenko LP, Coster AJ, Zhang SR et al (2018) Deep ionospheric hole created by sudden stratospheric warming in the nighttime ionosphere. J Geophys Res Sp Phys 123:7621–7633. https://doi.org/10.1029/2018JA025541

Gu SY, Liu HL, Dou X, Li T (2016) Influence of the sudden stratospheric warming on quasi-2-day waves. Atmos Chem Phys 16:4885–4896. https://doi.org/10.5194/acp-16-4885-2016

Hartmann DL (1983) Barotropic instability of the polar night jet stream. J Atmos Sci 40:817–835. https://doi.org/10.1175/1520-0469(1983)040%3c0817:BIOTPN%3e2.0.CO;2

He M, Chau JL, Stober G et al (2017) Application of manley-rowe relation in analyzing nonlinear interactions between planetary waves and the solar semidiurnal tide during 2009 sudden stratospheric warming event. J Geophys Res Sp Phys 122:10783–10795. https://doi.org/10.1002/2017JA024630

Hocking WK, Fuller B, Vandepeer B (2001) Real-time determination of meteor-related parameters utilizing modern digital technology. J Atmos Solar-Terrestrial Phys 63:155–169

Hoffmann P, Singer W, Keuer D et al (2007) Latitudinal and longitudinal variability of mesospheric winds and temperatures during stratospheric warming events. J Atmos Solar-Terrestrial Phys. https://doi.org/10.1016/j.jastp.2007.06.010

Holton JR (1980) The dynamics of sudden stratospheric warmings. Annu Rev Earth Planet Sci 8:169–190

Holton JR (1984) The generation of mesospheric planetary waves by zonally asymmetric gravity wave breaking. J Atmos Sci 41:3427–3430. https://doi.org/10.1175/1520-0469(1984)041%3c3427:TGOMPW%3e2.0.CO;2

Holton JR, Tan H-C (1980) The influence of the equatorial quasi-biennial oscillation on the global circulation at 50 mb. J Atmos Sci 37:2200–2208. https://doi.org/10.1175/1520-0469(1980)037%3c2200:TIOTEQ%3e2.0.CO;2

Holton JR, Tan H-C (1982) The quasi-biennial oscillation in the northern hemisphere lower stratosphere. J Meteorol Soc Japan Ser II 60:140–148. https://doi.org/10.2151/jmsj1965.60.1_140

John SR, Kumar KK (2016) Global normal mode planetary wave activity: a study using TIMED/SABER observations from the stratosphere to the mesosphere-lower thermosphere. Clim Dyn 47:3863–3881. https://doi.org/10.1007/s00382-016-3046-2

Karlsson B, McLandress C, Shepherd TG (2009) Inter-hemispheric mesospheric coupling in a comprehensive middle atmosphere model. J Atmos Solar-Terrestrial Phys 71:518–530. https://doi.org/10.1016/j.jastp.2008.08.006

Kishore Kumar G, Hocking WK (2010) Climatology of northern polar latitude MLT dynamics: mean winds and tides. Ann Geophys 28:1859–1876. https://doi.org/10.5194/angeo-28-1859-2010

Kishore Kumar G, Kishore Kumar K, Singer W et al (2014) Mesosphere and lower thermosphere zonal wind variations over low latitudes: relation to local stratospheric zonal winds and global circulation anomalies. J Geophys Res Atmos 119:5913–5927. https://doi.org/10.1002/2014JD021610

Körnich H, Becker E (2010) A simple model for the interhemispheric coupling of the middle atmosphere circulation. Adv Sp Res 45:661–668. https://doi.org/10.1016/j.asr.2009.11.001

Koushik N, Kumar KK, Ramkumar G, Subrahmanyam KV (2018) Response of equatorial and low latitude mesosphere lower thermospheric dynamics to the northern hemispheric sudden stratospheric warming events. J Atmos Solar-Terrestrial Phys 169:66–77. https://doi.org/10.1016/j.jastp.2018.01.021

Kumar KK, Subrahmanyam KV, Mathew SS et al (2018) Simultaneous observations of the quasi 2-day wave climatology over the low and equatorial latitudes in the mesosphere lower thermosphere. Clim Dyn 51:221–233. https://doi.org/10.1007/s00382-017-3916-2

Labitzke K (1971) Temperature changes in the Mesosphere and Stratoshere connected with circulation changes in winter. J Atmos Sci 29:756–766

Lima LM, Alves EO, Batista PP et al (2012) Sudden stratospheric warming effects on the mesospheric tides and 2-day wave dynamics at 7°S. J Atmos Solar-Terrestrial Phys 78–79:99–107. https://doi.org/10.1016/j.jastp.2011.02.013

Limpasuvan V, Orsolini YJ, Chandran A et al (2016) On the composite response of the MLT to major sudden stratospheric warming events with elevated stratopause. J Geophys Res Atmos 121:4518–4537. https://doi.org/10.1002/2015JD024401.Received

Liu HL, Roble RG (2002) A study of a self-generated stratospheric sudden warming and its mesospheric-lower thermospheric impacts using the coupled TIME-GCM/CCM3. J Geophys Res Atmos 107:1–18. https://doi.org/10.1029/2001JD001533

Matsuno T (1971) A dynamical model of the stratospheric sudden warming. J Atmos Sci 28:1479–1494

McCormack JP, Coy L, Hoppel KW (2009) Evolution of the quasi 2-day wave during January 2006. J Geophys Res Atmos 114:1–18. https://doi.org/10.1029/2009JD012239

Pancheva DV, Mukhtarov PJ, Mitchell NJ et al (2008) Planetary wave coupling (5–6-day waves) in the low-latitude atmosphere-ionosphere system. J Atmos Solar-Terrestrial Phys 70:101–122. https://doi.org/10.1016/j.jastp.2007.10.003

Paulino AR, Batista PP, Clemesha BR et al (2012) An enhancement of the lunar tide in the MLT region observed in the Brazilian sector during 2006 SSW. J Atmos Solar-Terrestrial Phys 90:97–103. https://doi.org/10.1016/j.jastp.2011.12.015

Pedatella NM, Forbes JM (2010) Evidence for stratosphere sudden warming-ionosphere coupling due to vertically propagating tides. Geophys Res Lett 37:1–5. https://doi.org/10.1029/2010GL043560

Plumb RA (1983) Baroclinic instability of the summer mesosphere: a mechanism for the quasi-two-day wave? J Atmos Sci 40:262–270. https://doi.org/10.1175/1520-0469(1983)040%3c0262:BIOTSM%3e2.0.CO;2

Portnyagin YI, Solovjova TV, Makarov NA et al (2004) Monthly mean climatology of the prevailing winds and tides in the Arctic mesosphere/lower thermosphere. Ann Geophys 22:3395–3410. https://doi.org/10.5194/angeo-22-3395-2004

Ramkumar G, Babu VS (2016) Climatology of horizontal winds in the lower and middle atmosphere over an equatorial station—Thiruvananthapuram. Curr Sci 111:500. https://doi.org/10.18520/cs/v111/i3/500-508

Riggin DM, Liu HL, Lieberman RS et al (2006) Observations of the 5-day wave in the mesosphere and lower thermosphere. J Atmos Solar-Terrestrial Phys 68:323–339. https://doi.org/10.1016/j.jastp.2005.05.010

Salby ML (1981) Rossby normal modes in nonuniform background configurations. Part II. Equinox and solstice conditions. J Atmos Sci 38:1827–1840. https://doi.org/10.1175/1520-0469(1981)038%3c1827:RNMINB%3e2.0.CO;2

Sassi F, Liu H (2014) Journal of atmospheric and solar-terrestrial physics westward traveling planetary wave events in the lower thermosphere during solar minimum conditions simulated by SD-WACCM-X. J Atmos Solar-Terrestrial Phys 119:11–26. https://doi.org/10.1016/j.jastp.2014.06.009

Sathishkumar S, Sridharan S (2009) Planetary and gravity waves in the mesosphere and lower thermosphere region over Tirunelveli (8.7??N, 77.8??E) during stratospheric warming events. Geophys Res Lett 36:1–5. https://doi.org/10.1029/2008GL037081

Sathishkumar S, Sridharan S (2013) Lunar and solar tidal variabilities in mesospheric winds and EEJ strength over Tirunelveli (8.7°N, 77.8°E) during the 2009 major stratospheric warming. J Geophys Res Sp Phys 118:533–541. https://doi.org/10.1029/2012JA018236

Schoeberl MR (1978) Stratospheric warmings: observation and theory. Rev Geophys 16:521–538

Shepherd MG, Wu DL, Fedulina IN et al (2007) Stratospheric warming effects on the tropical mesospheric temperature field. J Atmos Solar-Terrestrial Phys 69:2309–2337. https://doi.org/10.1016/j.jastp.2007.04.009

Siddiqui TA, Stolle C, Lühr H, Matzka J (2015) On the relationship between weakening of the northern polar vortex and the lunar tidal amplification in the equatorial electrojet. J Geophys Res A Sp Phys 120:10006–10019. https://doi.org/10.1002/2015JA021683

Siddiqui TA, Maute A, Pedatella N et al (2018) On the variability of the semidiurnal solar and lunar tides of the equatorial electrojet during sudden stratospheric warmings. Ann Geophys 36:1545–1562. https://doi.org/10.5194/angeo-36-1545-2018

Smith AK (1996) Longitudinal variations in mesospheric winds: evidence for gravity wave filtering by planetary waves. J Atmos Sci 53:1156–1173. https://doi.org/10.1175/1520-0469(1996)053%3c1156:LVIMWE%3e2.0.CO;2

Smith AK (1997) Stationary planetary waves in upper mesospheric winds. J Atmos Sci 54:2129–2145. https://doi.org/10.1175/1520-0469(1997)054%3c2129:SPWIUM%3e2.0.CO;2

Stray NH, Orsolini YJ, Espy PJ et al (2015) Observations of planetary waves in the mesosphere-lower thermosphere during stratospheric warming events. Atmos Chem Phys 15:4997–5005. https://doi.org/10.5194/acp-15-4997-2015

Tomikawa Y, Sato K, Watanabe S et al (2012) Growth of planetary waves and the formation of an elevated stratopause after a major stratospheric sudden warming in a T213L256 GCM. J Geophys Res Atmos 117:1–16. https://doi.org/10.1029/2011JD017243

Torrence C, Compo GP (1998) A practical guide to wavelet analysis. Bull Am Meteorol Soc 79:61–78. https://doi.org/10.1175/1520-0477(1998)079%3c0061:APGTWA%3e2.0.CO;2

Vineeth C, Kumar Pant T, Sridharan R (2009) Equatorial counter electrojets and polar stratospheric sudden warmings—a classical example of high latitude-low latitude coupling? Ann Geophys 27:3147–3153. https://doi.org/10.5194/angeo-27-3147-2009

Yadav S, Pant TK, Choudhary RK et al (2017) Impact of sudden stratospheric warming of 2009 on the equatorial and low-latitude ionosphere of the indian longitudes: a case study. J Geophys Res Sp Phys 122:10486–10501. https://doi.org/10.1002/2017JA024392

Yuan T, She CY, Krueger DA et al (2008) Climatology of mesopause region temperature, zonal wind, and meridional wind over Fort Collins, Colorado (41°N, 105°W), and comparison with model simulations. J Geophys Res Atmos 113:1–11. https://doi.org/10.1029/2007JD008697

Yuan T, Thurairajah B, She CY et al (2012) Wind and temperature response of midlatitude mesopause region to the 2009 sudden stratospheric warming. J Geophys Res Atmos 117:1–8. https://doi.org/10.1029/2011JD017142